

HYGROTHERMOELASTIC BUCKLING RESPONSE OF COMPOSITE LAMINATES BY USING MODIFIED SHEAR DEFORMATION THEORY

MASOUD KAZEMI

Environmental Sciences Research Center, Islamshahr Branch, Islamic Azad University, Islamshahr, Iran
e-mail: masoud_kazemi@hotmail.com; kazemii@iaau.ac.ir

In this study, a finite element based formulation is developed for analyzing the buckling and post-buckling of composite laminates subjected to mechanical and hygrothermal loads using Modified Hyperbolic Shear Deformation Theory (MHSDT). The changes in the critical buckling load are presented for different lamination schemes, thicknesses, material properties and plate aspect ratios. In addition, post buckling analysis is performed for a composite plate subjected to uniform in-plane thermal and moisture induced loadings by using MHSDT. Matlab software has been used for programming the analysis. The results obtained by Matlab codes are in a satisfactory consistence compared to the references. Thus, the developed MHSDT has been validated for buckling and post buckling analysis of laminated plates in hygrothermal environment.

Keywords: angle-ply laminate, buckling, composite plate, finite element method, shear deformation theory

1. Introduction

Compared to conventional metal structures, fibrous composite materials continue to experience increased application in aerospace, marine, automobile and other mechanical and civil structures due to their superior strength and stiffness to weight ratios; however, due to material anisotropy, analyzing and designing these materials are more complicated than metallic materials.

In order to prevent buckling and post-buckling effects in laminated plates, using an extra-strength is of great practical importance in the structural design of laminated plates.

Buckling is known as one of the most critical failure modes, often pre-generated or produced during service life. A significant reduction in weight of laminated plates can be achieved considering the post buckling behavior, which is an important factor in aerospace structures. The elastic buckling and post-buckling of fiber reinforced composite plates are investigated in several textbooks (Agarwal *et al.*, 2006; Reddy, 2004; Turvey and Marshall, 2012). Composite laminates are also susceptible to delamination buckling and exterior damage at stress free edges, which occurs when the properties mismatch at the ply interface. It can also be produced by external forces, elevated temperature and absorbed moisture. Stresses within laminates are redistributed to reduce the load carrying capacity, when delamination occurs. Composite laminates are subjected to changing environmental conditions like temperature and moisture. The effect of temperature and moisture is known as thermal and hygroscopic effect, respectively. The combined effect of these two parameters is called the hygrothermal effect. A hygrothermal environment reduces both strength and elastic properties, especially in the case of fibrous polymeric composites. Furthermore, associated hygrothermal expansion, either alone or in combination with mechanically produced deformation, can result in buckling, large deflections, and high stress levels. Consequently, examining the hygrothermal effects is essential in analyzing and designing laminated systems (Tauchert and Huang, 2012). Due to the fact that most applications are limited to purely thermal loadings, the majority of published researches lie in this field.

According to the similarities between mathematical formulations of the governing thermal and hygroscopic loadings, the given thermoelastic solutions could be generalized to elasto-hygrothermal cases. Similarly, it is not difficult to simplify the hygrothermal formulations and solution methods to include the isothermal effects. For predicting the real behavior of a structure, it is important to choose an adequate theory which is used in the expansion of different variables (Mantari *et al.*, 2012). In the 3D elasticity theory, heterogeneous laminated plates are modeled as 3D solid elements, so predicting transverse shear stresses can be significantly improved, however, by using this theory would lead to a complex procedure and multiplied computational cost.

In the literature, different models have been suggested for studying the composite laminated structures, including layerwise, quasi-layerwise and equivalent single layer models. Three principal equivalent theories have been proposed to reduce the 3D models to 2D ones; which are known as the Classical Laminated Plate Theory (CLPT), First-order Shear Deformation Theory (FSDT) and Higher-order Shear Deformation Plate Theory (HSDT) (Kharazi *et al.*, 2014).

In the CLPT, which relies on the Love-Kirchhoff assumptions, the transverse shear deformation is neglected and is only applicable for thin laminated plates, so, in order to consider the shear effect, the FSDT based on Reissner-Mindlin theory has been developed. The FSDT is simple to perform and can be applied for both thick and thin laminates; however, the accuracy of solutions strongly relies on the shear correction factors. In addition, the FSDT would not give satisfactory results in predicting the accurate and smooth variations of stresses, specifically for laminated plates with clamped or free edges, sharp corners and highly skewed geometry where high stress gradients occur. To overcome the limitation of the FSDT, a simple higher order theory was presented by Reddy (2004) for laminated plates, various types of HSDT, which include higher order terms in Taylor's expansion.

Many studies in the literature investigated the buckling and post-buckling in composite laminated thin plates subjected to mechanical or thermal loadings or both based on the classical plate theory, see for example (Kazemi and Verchery, 2016; Peković *et al.*, 2015; Ahmadi and Pourshahsavari, 2016; Muc and Chwał, 2016). In some other studies (Girish and Ramachandra, 2005; Mechab *et al.*, 2012; Dafedar and Desai, 2002), the application of shear deformation plate theories was developed for buckling and post-buckling analysis of laminated plates under combined mechanical and thermal loading. It should be noted that in all these investigations, the material properties are considered to be independent of temperature. Although comprehensive literature has been published in the field of pure mechanical or pure thermal loadings, few investigations have been devoted to the elastic buckling and post-buckling caused by coupled thermal and mechanical loads, which is encountered in real cases and operational life of composite structures.

A refined two-dimensional model was proposed by Brischetto (2013) for static hygrothermal analysis of laminated composites and sandwich shells neglecting the transverse shear deformation effects. Sreehari and Maiti (2015) introduced a finite element solution for handling buckling and post buckling analysis of laminated plates under mechanical and hygrothermal loads using a refined HSDT; however, the accuracy of the method was verified only for cross-ply laminates. Natarajan *et al.* (2014) considered the effect of moisture condensation and thermal variation on the vibration and buckling of laminates with cutouts within the formulation of the extended finite element method. Pandey *et al.* (2009) examined the influence of moisture concentration, temperature variation, plate parameters and fiber-volume fraction on the buckling and post buckling of the laminated plates based on HSDT and von Karman's nonlinear kinematics; however, the distribution of temperature and moisture on the surface was assumed to be uniform.

The aim of present work is to analyze the buckling and post buckling behavior of composite laminated plates in hygrothermal environment using the Finite Element Method (FEM) based on a new higher order formulation, in which the displacement of the middle surface is developed

as a trigonometric and exponential function of thickness, and the transverse displacement is assumed to be constant through the thickness. An appropriate distribution of the transverse shear strain is assumed across the plate thickness and, also, the stress-free boundary conditions are considered on the boundary surface, therefore, a shear modification factor is not needed.

2. Trigonometric shear displacement model (TSDM)

A laminated plate consisting of N orthotropic plies is considered. Length, width and thickness of the rectangular plate are a , b , and h , respectively. An 8-noded serendipity quadrilateral element, which is C^0 -continuous isoperimetric bi-quadratic, has been used for discretization of the laminated plate. In this work, the following new displacement model is proposed to satisfy the boundary conditions at the top and bottom of the laminated plate

$$\begin{aligned} u(x, y, z) &= u_0(x, y) - z \frac{\partial w}{\partial x} + \left[\sin \frac{\pi z}{h} \exp\left(m \cos \frac{\pi z}{h}\right) + \frac{\pi}{h} m z \right] \theta_x(x, y) \\ v(x, y, z) &= v_0(x, y) - z \frac{\partial w}{\partial y} + \left[\sin \frac{\pi z}{h} \exp\left(m \cos \frac{\pi z}{h}\right) + \frac{\pi}{h} m z \right] \theta_y(x, y) \\ w(x, y, z) &= w_0 \end{aligned} \quad (2.1)$$

where u , v , w represent displacement components in the x , y and z directions, respectively; and u_0 , v_0 , w_0 are displacement components in the middle surface of the plate. θ_x and θ_y are rotations about the y and x axes at the mid-plane, respectively. The first order derivatives of the transverse displacement can be formulated in terms of the in-plane displacement parameters as separate independent degrees of freedom as given below

$$\begin{aligned} u(x, y, z) &= u_0(x, y) - z \phi_x(x, y) + [g(z) + \Gamma z] \theta_x(x, y) \\ v(x, y, z) &= v_0(x, y) - z \phi_y(x, y) + [g(z) + \Gamma z] \theta_y(x, y) \\ w(x, y, z) &= w_0(x, y) \end{aligned} \quad (2.2)$$

where

$$\phi_x = \frac{\partial w}{\partial x} \quad \phi_y = \frac{\partial w}{\partial y} \quad g(z) = \sin \frac{\pi z}{h} \exp\left(m \cos \frac{\pi z}{h}\right) \quad \Gamma = \frac{\pi}{h} m$$

The linear displacement vector given in the above equation can be expressed in terms of the middle surface of the laminated plate as follows

$$\boldsymbol{\varepsilon}_{5 \times 1} = \mathbf{Z}_{5 \times 13} \bar{\boldsymbol{\varepsilon}}_{13 \times 1} \quad (2.3)$$

where

$$\begin{aligned} \bar{\boldsymbol{\varepsilon}} &= \left\{ \varepsilon_1^0 \quad \varepsilon_2^0 \quad \varepsilon_6^0 \quad \kappa_1^1 \quad \kappa_2^1 \quad \kappa_6^1 \quad \varepsilon_4^0 \quad \varepsilon_5^0 \quad \kappa_4^2 \quad \kappa_5^2 \right\}^T \\ \varepsilon_1^0 &= \frac{\partial u_0}{\partial x} \quad \varepsilon_2^0 = \frac{\partial v_0}{\partial y} \quad \varepsilon_6^0 = \frac{\partial u_0}{\partial y} + \frac{\partial v_0}{\partial x} \quad \varepsilon_4^0 = \frac{\partial w_0}{\partial y} - \phi_y \\ \varepsilon_5^0 &= \frac{\partial w_0}{\partial x} - \phi_x \quad k_1^0 = \Gamma \frac{\partial \theta_x}{\partial x} - \frac{\partial \phi_x}{\partial x} \quad k_2^0 = \Gamma \frac{\partial \theta_y}{\partial y} - \frac{\partial \phi_y}{\partial y} \\ k_6^0 &= \Gamma \left(\frac{\partial \theta_x}{\partial y} + \frac{\partial \theta_y}{\partial x} \right) - \frac{\partial \phi_x}{\partial y} - \frac{\partial \phi_y}{\partial x} \quad k_1^1 = \frac{\partial \theta_x}{\partial x} \quad k_2^1 = \frac{\partial \theta_y}{\partial x} \\ k_6^1 &= \frac{\partial \theta_y}{\partial x} + \frac{\partial \theta_x}{\partial y} \quad k_4^2 = \theta_y \quad k_5^2 = \theta_x \end{aligned}$$

$$\mathbf{Z} = \begin{bmatrix} 1 & 0 & 0 & z & 0 & 0 & g(z) & 0 & 0 & 0 & 0 & 0 & 0 \\ 0 & 1 & 0 & 0 & z & 0 & 0 & g(z) & 0 & 0 & 0 & 0 & 0 \\ 0 & 0 & 1 & 0 & 0 & z & 0 & 0 & 0 & g(z) & 0 & 0 & 0 \\ 0 & 0 & 0 & 0 & 0 & 0 & 0 & 0 & 0 & 1 & 0 & g(z) & 0 \\ 0 & 0 & 0 & 0 & 0 & 0 & 0 & 0 & 0 & 0 & 1 & 0 & g(z) \end{bmatrix}$$

and

$$\bar{\boldsymbol{\varepsilon}}_{13 \times 1} = \mathbf{L}_{13 \times 7} \boldsymbol{\Delta}_{7 \times 1} \quad \boldsymbol{\Delta} = \{u_0 \quad v_0 \quad w_0 \quad \theta_x \quad \theta_y \quad \phi_x \quad \phi_y\}^T$$

The following assumptions are considered in the derivation of the equations:

- Small elastic deformations are assumed (i.e. deformations and rotations are small and agree to the Hooke's law).
- The plies of the composite laminated structure are supposed to be well bonded.

The linear strain equations derived from the displacements of Eqs. (2.1), which are valid for thin as well as thick plates under consideration, are as follows

$$\begin{aligned} \varepsilon_{xx} &= \varepsilon_{xx}^0 + z\varepsilon_{xx}^1 + \sin \frac{\pi z}{h} \exp\left(m \cos \frac{\pi z}{h}\right) \varepsilon_{xx}^2 \\ \varepsilon_{yy} &= \varepsilon_{yy}^0 + z\varepsilon_{yy}^1 + \sin \frac{\pi z}{h} \exp\left(m \cos \frac{\pi z}{h}\right) \varepsilon_{yy}^2 \\ \varepsilon_{xy} &= \varepsilon_{xy}^0 + z\varepsilon_{xy}^1 + \sin \frac{\pi z}{h} \exp\left(m \cos \frac{\pi z}{h}\right) \varepsilon_{xy}^2 \\ \varepsilon_{xz} &= \varepsilon_{xz}^0 + \frac{\pi}{h} \left(\cos \frac{\pi z}{h} - m \sin^2 \frac{\pi z}{h}\right) \exp\left(m \cos \frac{\pi z}{h}\right) \varepsilon_{xz}^3 \\ \varepsilon_{yz} &= \varepsilon_{yz}^0 + \frac{\pi}{h} \left(\cos \frac{\pi z}{h} - m \sin^2 \frac{\pi z}{h}\right) \exp\left(m \cos \frac{\pi z}{h}\right) \varepsilon_{yz}^3 \end{aligned} \quad (2.4)$$

and

$$\begin{aligned} \varepsilon_{xx}^0 &= \frac{\partial u}{\partial x} & \varepsilon_{xx}^1 &= m \frac{\pi}{h} \frac{\partial \theta_x}{\partial x} - \frac{\partial^2 w}{\partial x^2} & \varepsilon_{xx}^2 &= \frac{\partial \theta_x}{\partial x} \\ \varepsilon_{yy}^0 &= \frac{\partial v}{\partial x} & \varepsilon_{yy}^1 &= m \frac{\pi}{h} \frac{\partial \theta_y}{\partial x} - \frac{\partial^2 w}{\partial x^2} & \varepsilon_{yy}^2 &= \frac{\partial \theta_y}{\partial x} \\ \varepsilon_{xy}^0 &= \frac{\partial v}{\partial x} + \frac{\partial u}{\partial y} & \varepsilon_{xy}^1 &= m \frac{\pi}{h} \frac{\partial \theta_y}{\partial x} + m \frac{\pi}{h} \frac{\partial \theta_x}{\partial y} - 2 \frac{\partial^2 w}{\partial x \partial y} & \varepsilon_{xy}^2 &= \frac{\partial \theta_y}{\partial x} + \frac{\partial \theta_x}{\partial y} \\ \varepsilon_{xz}^0 &= m \frac{\pi}{h} \theta_x & \varepsilon_{xz}^3 &= \theta_x & \varepsilon_{yz}^0 &= m \frac{\pi}{h} \theta_y & \varepsilon_{yz}^3 &= \theta_y \end{aligned} \quad (2.5)$$

3. Governing equations of the hygrothermal buckling and post-buckling

The laminated plate composed of elastic orthotropic plies and the stress-strain relations in the orthotropic local frame are as follows (Reddy, 2004)

$$\begin{Bmatrix} \sigma_1 \\ \sigma_2 \\ \tau_{12} \\ \tau_{13} \\ \tau_{23} \end{Bmatrix} = \begin{bmatrix} Q_{11} & Q_{12} & 0 & 0 & 0 \\ Q_{12} & Q_{22} & 0 & 0 & 0 \\ 0 & 0 & Q_{66} & 0 & 0 \\ 0 & 0 & 0 & Q_{55} & 0 \\ 0 & 0 & 0 & 0 & Q_{44} \end{bmatrix} \begin{Bmatrix} \varepsilon_1 \\ \varepsilon_2 \\ \gamma_{12} \\ \gamma_{13} \\ \gamma_{23} \end{Bmatrix} \quad (3.1)$$

where Q_{ij} are elastic stiffness coefficients relative to the plane-stress state that neglects the transversal stress. These coefficients are given below (Reddy, 2004) in terms of the engineering constants in the material coordinates

$$\begin{aligned}
Q_{11} &= \frac{E_1}{1 - \nu_{12}\nu_{21}} & Q_{22} &= \frac{E_2}{1 - \nu_{12}\nu_{21}} & Q_{12} &= \nu_{12}Q_{11} & Q_{33} &= G_{12} \\
Q_{44} &= G_{23} & Q_{55} &= G_{13} & \nu_{21} &= \nu_{12}\frac{E_2}{E_1}
\end{aligned} \tag{3.2}$$

In general, the laminates are in the plane stress state due to temperature or moisture changes; therefore, externally applied stresses would develop at the supports. These in-plane stresses can be evaluated using elasto-hygrothermal constitutive equation. When hygrothermal effects are considered, the stress tensor is usually expressed in the contracted notation as follows

$$\sigma_i = Q_{ij} \left(\varepsilon_j - \int_{T_0}^T \alpha_j(\tau, M) d\tau - \int_{M_0}^M \beta_j(T, m) dm \right) \quad i, j = 1, 2, 3 \tag{3.3}$$

where the elastic stiffness coefficients Q_{ij} , the thermal expansion coefficients α_j , and the moisture coefficients β_j depend upon the temperature T and moisture concentration M . For moderate temperature $\Delta T = T - T_0$ and moisture $\Delta M = M - M_0$ changes from the corresponding stress-free values T_0 and M_0 , if the elastic properties are considered independent from the hygrothermal, the stress-strain relations are simplified as follows

$$\sigma = Q_{ij}(\varepsilon_1 - \alpha_j \Delta T - \beta \Delta M)(\varepsilon_1 - \alpha_j \Delta T - \beta \Delta M) \quad i, j = 1, 2, 3 \tag{3.4}$$

Proper tensor transformations can be employed in transforming equation (3.4) from principal material coordinates x_1, x_2 and x_3 to the plate coordinates x, y and z . For a typical k -th ply of the laminate, the resulted expression can be written as

$$\left\{ \begin{array}{l} \sigma_{xx} \\ \sigma_{yy} \\ \tau_{xy} \\ \tau_{xz} \\ \tau_{yz} \end{array} \right\}_k = \left[\begin{array}{ccccc} \bar{Q}_{11} & \bar{Q}_{12} & \bar{Q}_{16} & 0 & 0 \\ \bar{Q}_{12} & \bar{Q}_{22} & \bar{Q}_{26} & 0 & 0 \\ \bar{Q}_{16} & \bar{Q}_{26} & \bar{Q}_{66} & 0 & 0 \\ 0 & 0 & 0 & \bar{Q}_{55} & \bar{Q}_{54} \\ 0 & 0 & 0 & \bar{Q}_{45} & \bar{Q}_{44} \end{array} \right]_k \left\{ \begin{array}{l} \varepsilon_{xx} - \alpha_x \Delta T - \beta_x \Delta C \\ \varepsilon_{yy} - \alpha_y \Delta T - \beta_y \Delta C \\ \varepsilon_{xy} - \alpha_{xy} \Delta T - \beta_{xy} \Delta C \\ \varepsilon_{xz} \\ \varepsilon_{yz} \end{array} \right\}_k \tag{3.5}$$

or in a condensed form

$$\sigma_k = \bar{Q}_k \varepsilon_k \tag{3.6}$$

where $\bar{Q}_{ij}, \alpha_i, \beta_i$ ($i, j = x, y, xy$) denote the transformed material coefficients.

According to the potential energy theorem, the equilibrium state can be achieved when variation of the total potential energy equates to zero.

The potential energy theorem can be expressed for the typical i -th ply enclosing a space volume V as follows

$$\int_V (\sigma_{xx} \delta \varepsilon_{xx} + \sigma_{yy} \delta \varepsilon_{yy} + \tau_{xy} \delta \varepsilon_{xy} + \tau_{xz} \delta \varepsilon_{xz} + \tau_{yz} \delta \varepsilon_{yz}) dV_e - \int_A q \delta w dA_e = 0 \tag{3.7}$$

When the laminate is subjected to temperature or moisture changes, due to the restriction on freeing the hygrothermal loading, some stresses are developed at the supports. The governing equations on the pre-buckling can be obtained via the following formula

$$\mathbf{K} \Delta = \mathbf{F} \tag{3.8}$$

where \mathbf{K} is the linear stiffness matrix and \mathbf{F} represents the load vector associated with the temperature variation or hygroscopic effects. Equation (3.8) is solved under the specified boundary condition and in-plane loads. In the next step, the geometric stiffness matrix \mathbf{K}_G associated

with these in-plane loads is calculated. The critical hygrothermal buckling is calculated through solving the linear eigenvalue problem

$$(\mathbf{K} + \lambda_{cr}\mathbf{K}_G)\mathbf{\Delta} = \mathbf{0} \quad (3.9)$$

The smallest eigenvalue corresponds to the amplitude of the critical buckling load. In the post-buckling step, the nonlinear stiffness matrix \mathbf{K}_{nl} is incorporated as

$$(\mathbf{K} + \mathbf{K}_{nl} + \lambda_{cr}\mathbf{K}_G)\mathbf{\Delta} = \mathbf{0} \quad (3.10)$$

The geometric stiffness matrix can be expressed as

$$\mathbf{K}_G = \sigma_x^p\mathbf{K}_{G1} + \sigma_y^p\mathbf{K}_{G2} \quad (3.11)$$

where σ_x^p , σ_y^p denote externally applied stresses acting in the x and y directions. Subsequently, the critical buckling stresses can be calculated by the following formulas

$$\sigma_{xc}^p r = \lambda_{cr}\sigma_x^p \quad \sigma_{yc}^p r = \lambda_{cr}\sigma_y^p \quad (3.12)$$

4. Numerical results and discussion

In this Section, numerical examples are presented for buckling and post buckling of the laminated composite plates under mechanical and hygrothermal loads. The accuracy of the proposed TSDM model considering the transverse shear stresses is examined. A variety of problems are solved using the finite element formulation and the results are compared with 3D elasticity solution. It is important to note that the proposed displacement model can be applied to any lay-up of the laminated plates. The different mechanical properties examined in the numerical examples are given in Table 1.

Table 1. Material properties used in the numerical examples

Material No.	Elastic constants (Reddy and Liu, 1985; Dafedar and Desai, 2002)							
	1	$E_1/E_2 = 25$, $G_{12} = G_{13} = 0.5E_2$, $G_{23} = 0.2E_2$, $\nu_{12} = 0.25$						
2	$E_1/E_2 = 3$ to 40 , $E_3 = E_2$, $G_{12}/E_2 = G_{13}/E_2 = 0.60$, $G_{23}/E_2 = 0.50$, $\nu_{12} = \nu_{23} = \nu_{13} = 0.25$							
3	$E_1/E_2 = 40$, $E_3 = E_2$, $G_{12}/E_2 = G_{13}/E_2 = 0.50$, $G_{23}/E_2 = 0.20$, $\nu_{12} = \nu_{23} = \nu_{13} = 0.25$							
4	$E_1/E_2 = 15$, $E_3 = E_2$, $G_{12}/E_2 = G_{13}/E_2 = 0.50$, $G_{23}/E_2 = 0.3356$, $\nu_{12} = \nu_{23} = \nu_{13} = 0.3$, $a_1/a_0 = 0.015$, $a_2/a_0 = a_3/a_0 = 1.00$							
5	Elastic moduli of graphite/epoxy ply at different moisture concentrations C [%], $E_1 = 130$ GPa, $G_{13} = G_{12} = 6.0$ GPa, $G_{23} = 0.5G_{12}$, $\nu_{12} = \nu_{23} = \nu_{13} = 0.3$, $\beta_1 = 0$ and $\beta_2 = \beta_3 = 0.44$ and							
	C [%]	0.00	0.25	0.50	0.75	1.00	1.25	1.50
	E_2 [GPa]	9.50	9.25	9.00	8.75	8.50	8.50	8.50

In order to simplify comparison, the critical buckling stresses have been transformed into dimensionless coefficients as follows

$$\lambda_{cr} = \frac{\sigma_{cr}b^2}{E_2h^2} \quad (4.1)$$

4.1. Examples for validating the TSDM model

Three cases are examined to confirm TSDM formulation using finite element programming.

Case A

A symmetric four-layered (0/90/90/0) cross-ply laminated plate is considered under uniaxial compression loading. The critical buckling coefficients for various values of length-to-thickness ratios a/h are presented in Table 2. As it is demonstrated in Table 2, the HSDT overestimates the critical buckling loads in comparison with the results from the present formulation and those given by Pagano *et al.* (1994).

Table 2. Effect of length to thickness ratio on the critical buckling load

a/h	Present	3D (Pagano and Reddy, 1994)	HSDT (Reddy and Liu, 1985)
5	1.922	1.575	1.997
10	13.367	13.453	13.384
20	20.689	21.707	21.886
50	23.354	23.356	23.747
100	24.034	24.255	24.953

Case B

The effect of elastic moduli ratios on the buckling loads of a square plate under uniaxial loading is examined, and the results are presented in Table 3. According to the results obtained via the TSDM formulation are in excellent agreement with other references.

Table 3. Effect of elastic moduli ratios on critical buckling loads

E_1/E_2	Present	3D (Pagano and Reddy, 1994)	HSDT (Reddy and Liu, 1985)
3	5.396	5.399	5.114
10	9.952	9.967	13.384
20	15.327	15.352	15.297
30	19.703	19.758	19.968
40	23.564	23.451	23.344

Case C

Table 4 presents the comparison between the critical buckling coefficients obtained through the present model and the reference values for the square laminated plate under uniaxial compression loading. The analysis is carried out for two values of fiber orientation angles $\theta = 30^\circ$ and $\theta = 45^\circ$ for both of the two-ply and six-ply antisymmetric angle-ply laminates. The results are validated by comparing them with the HSDT model proposed by Reddy and Liu (1985).

4.2. Effect of the length-to-thickness ratio on the critical buckling load

A symmetric four-layered (0/90)s cross-ply laminated plate is considered under both uniaxial and biaxial compression loadings. The effect of the side-to-thickness ratio for the simply supported rectangular plate is examined using material No. 1, and the results are plotted in Fig.1. It is

Table 4. Critical buckling coefficients for angle-ply laminates

$\theta = 30^\circ$					$\theta = 45^\circ$				
a/h	2 ply		6 ply		a/h	2 ply		6 ply	
	Present	[10]	Present	[10]		Present	[10]	Present	[10]
5	10.694	11.543	13.404	13.536	5	10.084	10.782	12.169	12.172
10	16.108	17.123	29.046	33.624	10	16.734	18.051	30.648	32.504
20	18.234	18.764	41.023	46.231	20	19.234	19.764	48.230	52.132
50	19.748	19.863	49.963	51.643	50	20.746	20.863	58.963	59.643
100	20.308	30.603	53.079	54.896	100	21.267	21.664	59.431	61.021

[10] – Muc and Chwał (2016)

observed that the critical buckling loads are higher in the uniaxial loading case. Additionally, the buckling load coefficients increase considerably as the thickness ratio decreases. The variations of both curves for two loading conditions are very slow above the $a/h = 40$ ratio (are only a little above $a/h = 40$).

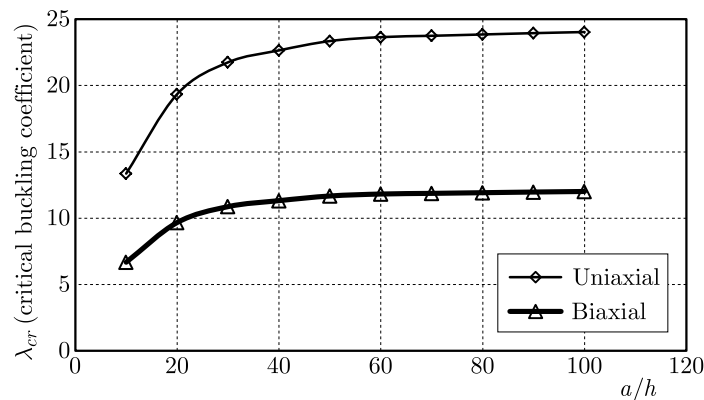


Fig. 1. Effect of the length-to-thickness ratio on the critical buckling load for cross-ply laminates

4.3. Effect of ply orientation on the critical buckling load

The buckling load coefficient for a square and antisymmetric angle-ply laminated plate is tested under uniaxial compressive loading; the effect of ply orientation for various numbers of layers of the angle-ply laminate is plotted in Fig. 2. All the edges are supposed to be simply supported, and material 5 of Table 1 is used in all cases. It is observed that in all cases, the

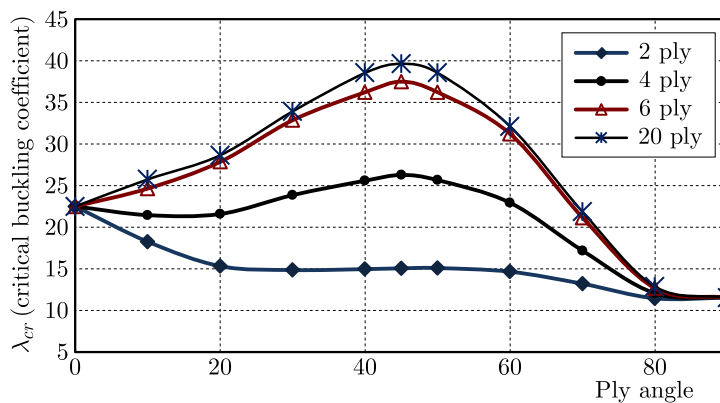


Fig. 2. Effect of the ply angle on the critical buckling load

critical buckling load increases at first but decreases then. By varying the fiber orientation angles from 0° to 90° , it is observed that the maximum critical buckling load occurs at 45° .

4.4. Effect of the elastic moduli ratio on the critical buckling load

The variations of critical buckling coefficients of antisymmetric cross-ply laminated plates under uniaxial and biaxial loadings are demonstrated in Figs. 3, respectively. The results are presented for $a/h = 10$. It is observed that as the elastic moduli ratio rises, the critical buckling load also increases in both uniaxial and biaxial loadings; however, in biaxial cases, the buckling loads are approximately half of the corresponding uniaxial values at all analyzed ratios.

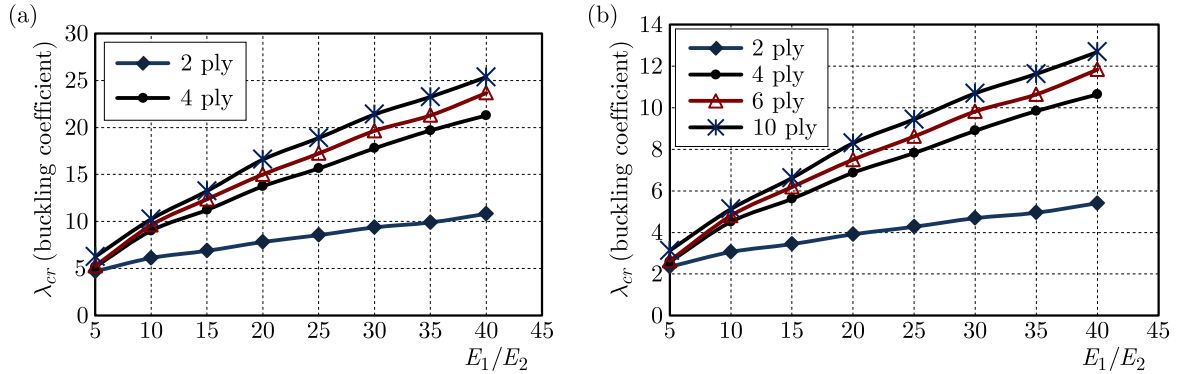


Fig. 3. Variation of the buckling load for square antisymmetric cross-ply laminate when $a/h = 10$; (a) uniaxial loading, (b) biaxial loading

4.5. Effect of thermal loads on the buckling of laminates

Buckling under thermal loads for a laminated plate consisting of 10 plies of material 4 is examined using TSDM model and compared with 3D elasticity solutions. The thermal buckling coefficients of $\lambda_T = \alpha_0 T_{cr}$ are provided in Table 5. The obtained results are in excellent agreement with the 3D elasticity results proposed by Noor and Burton (1992), for both the thin and thick laminated plates. In this case, the critical buckling loads correspond to the buckling modes of $m, n = 1, 2$, because the laminates under high temperature variations are mainly subjected to the biaxial loading condition. The results confirm that the buckling in the thick laminated plates occur at higher temperatures compared to the thin ones. In Fig. 4, the thermo-buckling curve is plotted for a simply supported square and $[\pm 45^\circ]$ antisymmetric angle-ply laminate. The obtained results by the present model are very close to the analytical solutions proposed by Singha *et al.* (2001).

Table 5. Thermal buckling coefficient $\lambda_T = \alpha_0 T_{cr}$ for a square angle-ply laminated plate

a/h	Present	3D solution (Noor and Burton, 1992)
100.0000	$0.7463 \cdot 10^{-3}$	$0.7458 \cdot 10^{-3}$
20.0000	$0.1739 \cdot 10^{-3}$	$0.1721 \cdot 10^{-3}$
10.0000	$0.5782 \cdot 10^{-3}$	$0.5820 \cdot 10^{-3}$
6.6667	0.1029	0.1034
5.0000	0.1436	0.1515
4.0000	0.1777	0.1886
3.3333	0.2057	0.2063

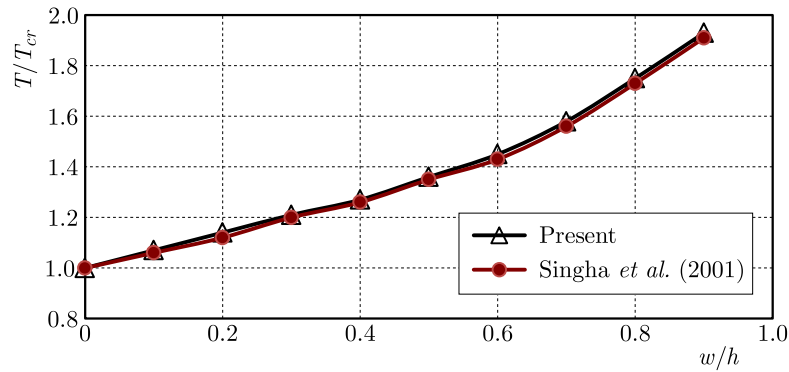


Fig. 4. Thermo-buckling path plotted for a simply supported square $[\pm 45^\circ]$ antisymmetric angle-ply laminate

4.6. Effect of change in moisture concentration on the buckling load

The effects of changes in moisture concentrations on the uniaxial buckling load coefficients λ_U of a cross-ply $[(0/90)_s]$ laminate using material 5 is presented in Table 6. The buckling loads are evaluated by reducing the material properties and increasing the moisture concentration. The parameter $(E_2)_{c=0\%}$ is used to calculate the buckling load coefficient λ_U using the TSDM model. In Fig. 6, the variation of the buckling load coefficient with respect to the moisture concentration is shown for different b/h ratios. As it is seen from this figure, in thin plates, the buckling coefficient decreases faster compared to the thick ones. However, the slope is almost linear for both thin and thick laminates, and the thin plates may buckle due to a little change in the moisture concentration, even in the absence of external loads.

Table 6. Effect of moisture concentration on the critical buckling load coefficient of a symmetric cross-ply laminated plate for various values of the thickness-to-length ratio

a/h	C [%]	Present	Dafedar and Desai (2002)
5	0.0	6.9932	7.1383
	0.5	6.8911	7.0365
	1.0	6.7963	6.9420
	1.5	6.7320	6.8776
10	0.0	11.3466	11.4275
	0.5	11.0183	11.0990
	1.0	10.7205	10.8009
	1.5	10.4631	10.5435
20	0.0	13.6835	13.7106
	0.5	12.5247	12.5517
	1.0	11.4879	11.5147
	1.5	10.4582	10.4851
40	0.0	14.4529	14.4602
	0.5	10.0180	10.0254
	1.0	6.0708	6.0781
	1.5	1.9523	1.9596

5. Conclusions

A new finite element formulation is developed using MHSMT for investigating the effects of elasto-hygrothermal loads in the buckling of composite laminated plates. The transverse stresses through thickness of a plate and the continuity of displacements are entirely satisfied in the proposed formulation. From the extensive numerical investigation, the results obtained using Trigonometric Shear Displacement Model (TSDM) is in excellent agreement with the three-dimensional elasticity solutions as well as other equivalent higher-order theories. The variations of the critical buckling load are presented for different lamination lay-ups, elastic constants and length-to-thickness plate ratios. The effect of thermally-induced loading and moisture concentration on the buckling and post-buckling of the laminated plates are investigated using TSDM formulation. The following conclusions are obtained:

- In the hygrothermal buckling analysis of composite plates, it is mandatory to exploit refined higher-order theories dealing with the transverse normal deformation.
- Increasing the moisture concentrations and temperatures would result in a reduction in the buckling and post-buckling strength. The results also confirm that the post-buckling characteristics are significantly affected by a rise in the temperature, moisture concentration, transverse shear deformation, plate geometry, total number of plies and fiber orientation.
- Increasing the length-to-thickness ratio, the number of layers and the orthotropic ratio (E_1/E_2) would lead to an increase in the buckling strength due to in-plane compressive loading.
- The critical buckling load is higher in the case of uniaxial loading compared to the biaxial one.

References

1. AGARWAL B.D., BROUTMAN L.J., CHANDRASHEKHARA K., 2006, *Analysis and Performance of Fiber Composites*, 3rd ed., Wiley, New York
2. AHMADI S.A., POURSHAHAVARI H., 2016, Three-dimensional thermal buckling analysis of functionally graded cylindrical panels using differential quadrature method (DQM), *Journal of Theoretical and Applied Mechanics*, **54**, 1, 135-147
3. BRISCHETTO S., 2013, Hygrothermoelastic analysis of multilayered composite and sandwich shells, *Journal of Sandwich Structures and Materials*, **15**, 2, 168-202
4. DAFEDAR J.B., DESAI Y.M., 2002, Thermomechanical buckling of laminated composite plates using mixed, higher-order analytical formulation, *Journal of Applied Mechanics*, **69**, 6, 790-799
5. GIRISH J., RAMACHANDRA L.S., 2005, Thermomechanical post-buckling analysis of symmetric and antisymmetric composite plates with imperfections, *Composite Structures*, **67**, 4, 453-460
6. KAZEMI M., VERCHERY G., 2016, Design of composite laminated plates for maximum buckling load with stiffness and elastic modulus constraints, *Composite Structures*, **148**, 27-38
7. KHARAZI M., OVESY H.R., MOONEGHI M.A., 2014, Buckling analysis of delaminated composite plates using a novel layerwise theory, *Thin-Walled Structures*, **74**, 246-254
8. MANTARI J.L., OKTEM A.S., SOARES C.G., 2012, A new higher order shear deformation theory for sandwich and composite laminated plates, *Composites Part B: Engineering*, **43**, 3, 1489-1499
9. MECHAB B., MECHAB I., BENAÏSSA S., 2012, Analysis of thick orthotropic laminated composite plates based on higher order shear deformation theory by the new function under thermo-mechanical loading, *Composites Part B: Engineering*, **43**, 3, 1453-1458

10. MUC A., CHWAŁ M., 2016, Analytical discrete stacking sequence optimization of rectangular composite plates subjected to buckling and FPF constraints, *Journal of Theoretical and Applied Mechanics*, **54**, 2, 423-436
11. NATARAJAN S., DEOGEKAR P.S., MANICKAM G., BELOUETTAR S., 2014, Hygrothermal effects on the free vibration and buckling of laminated composites with cutouts, *Composite Structures*, **108**, 848-855
12. NOOR A.K., BURTON W.S., 1992, Three-dimensional solutions for thermal buckling of multilayered anisotropic plates, *Journal of Engineering Mechanics*, **118**, 4, 683-701
13. PAGANO N.J., REDDY J.N., 1994, *Mechanics of Composite Materials: Selected Works of Nicholas J. Pagano*, **34**, Springer Science & Business Media
14. PANDEY R., UPADHYAY A.K., SHUKLA K.K., 2009, Hygrothermoelastic postbuckling response of laminated composite plates, *Journal of Aerospace Engineering*, **23**, 1, 1-13
15. PEKOVIĆ O., STUPAR S., SIMONOVIĆ A., SVORCAN J., TRIVKOVIĆ S.A., 2015, Free vibration and buckling analysis of higher order laminated composite plates using the isogeometric approach, *Journal of Theoretical and Applied Mechanics*, **53**, 2, 453-466
16. REDDY J.N., LIU C.F., 1985, A higher-order shear deformation theory of laminated elastic shells, *International Journal of Engineering Science*, **23**, 3, 319-330
17. REDDY J.N., 2004, *Mechanics of Laminated Composite Plates and Shells*, 2nd ed., CRC Press
18. SINGHA M.K., RAMACHANDRA L.S., BANDYOPADHYAY J.N., 2001, Thermal post-buckling analysis of laminated composite plates, *Composite Structures*, **54**, 4, 453-458
19. SREEHARI V.M., MAITI D.K., 2015, Buckling and post buckling analysis of laminated composite plates in hygrothermal environment using an Inverse Hyperbolic Shear Deformation Theory, *Composite Structures*, **129**, 250-255
20. TAUCHERT T., HUANG N., 2012, Laminated Plates, *Composite Structures 4: Volume 1 Analysis and Design Studies*, 424
21. TURVEY G.J., MARSHALL I.H., EDS., 2012, *Buckling and Postbuckling of Composite Plates*, Springer Science & Business Media, Netherlands

Manuscript received March 30, 2017; accepted for print June 7, 2017